

# Infrared Multiple Photon Dissociation Spectra of Proton- and Sodium Ion-Bound Glycine Dimers in the N–H and O–H Stretching Region

Chad G. Atkins, Khadijeh Rajabi, Elizabeth A. L. Gillis, and Travis D. Fridgen\*

Department of Chemistry, Memorial University of Newfoundland, St. John's, Newfoundland and Labrador, Canada A1N 4T8

Received: June 23, 2008; Revised Manuscript Received: August 12, 2008

The proton- and the sodium ion-bound glycine homodimers are studied by a combination of infrared multiple photon dissociation (IRMPD) spectroscopy in the N–H and O–H stretching region and electronic structure calculations. For the proton-bound glycine dimer, in the region above  $3100\text{ cm}^{-1}$ , the present spectrum agrees well with one recorded previously. The present work also reveals a weak, broad absorption spanning the region from  $2650$  to  $3300\text{ cm}^{-1}$ . This feature is assigned to the strongly hydrogen-bonded and anharmonic N–H and O–H stretching modes. As well, the shared proton stretch is observed at  $2440\text{ cm}^{-1}$ . The IRMPD spectra for the proton-bound glycine dimer confirms that the lowest energy structure is an ion–dipole complex between N-protonated glycine and the carboxyl group of the second glycine. This spectrum also helps to eliminate the existence of any of the higher-energy structures considered. The IRMPD spectrum for the sodium ion-bound dimer is a much simpler spectrum consisting of three bands assigned to the O–H stretch and the asymmetric and symmetric  $\text{NH}_2$  stretching modes. The positions of these bands are very similar to those observed for the proton-bound glycine dimer. Numerous structures were considered and the experimental spectrum agrees with the B3LYP/6-31+G(d,p) predicted spectrum for the lowest energy structure, two bidentate glycine molecules bound to  $\text{Na}^+$ . Though some of the structures cannot be completely ruled out by comparing the experimental and theoretical spectra, they are energetically disfavored by at least  $20\text{ kJ mol}^{-1}$ .

## 1. Introduction

It has been well documented that neutral amino acids in the condensed phase are zwitterionic<sup>1</sup> whereas in matrix isolation experiments<sup>2</sup> or in the gas phase,<sup>3–5</sup> the nonzwitterionic form is dominant. Previous work on gaseous neutral glycine has shown that its zwitterion is not even a local minimum on its potential energy surface.<sup>6</sup> However, recent studies have investigated ways to induce the isomerization of gas phase amino acids from their neutral nonzwitterionic form to their zwitterionic state. Jensen et al.<sup>7</sup> introduced an approach whereby the addition of water molecules to such systems could aid the transition, and they demonstrated that a local minimum for the glycine zwitterion is created through interactions with two water molecules. From this success, further attempts were made to mimic an aqueous solution with the intention of favoring the zwitterionic form. This concept of microsolvation<sup>8–10</sup> continues to remain a prominent interest for the hydration chemistry of various gas phase systems.

Protonation reactions, shown to be vital for biological processes such as enzyme catalysis,<sup>11</sup> can occur in aqueous solutions containing amino acids and alter the system's conformational structure. Gaseous protonated amino acids (including protonated clusters),<sup>12–16</sup> those which are metal-cation associated,<sup>16–19</sup> or radical cations<sup>20</sup> have received much attention recently from the viewpoint of structure and thermochemistry. Such information is important for a clear understanding of a variety of biological processes. Comparing *ab initio* and/or density functional theory (DFT) calculations with experimental results obtained through infrared multiple-photon dissociation (IRMPD) can provide information such that structures can be

determined and evaluated. IRMPD spectroscopy has also been used very recently to investigate the effect of alkali cation size on producing a stable salt bridge (zwitterionic) form as opposed to a charge solvated (canonical) version.<sup>21–24</sup> The preference for charge solvation is believed to be reduced by a strong electrostatic interaction created between the metal cation and the dipole of the zwitterion. Earlier blackbody induced radiative dissociation (BIRD) studies have indicated that the addition of smaller cations to arginine favors charge solvated conformations, whereas the addition of larger metals stabilizes the salt bridge conformer.<sup>25</sup> BIRD studies also showed that only a few water molecules were necessary for alkali metal ion-bound valine<sup>26,27</sup> to adopt the zwitterionic structure. In a similar fashion, Bush et al.<sup>28</sup> most recently discovered that when lithiated arginine cation complexes with a single water molecule the zwitterion is the favored structure. Although these examples have revolved around the addition of alkali cations, it has previously been demonstrated that the study of proton-bound dimers can also provide interesting insight into this amino acid isomerization. Rajabi and Fridgen<sup>29</sup> found that the homogeneous proton-bound dimers of glycine, alanine and valine, as well as the mixed glycine/alanine proton bound dimer were nonzwitterionic. Furthermore, they demonstrated through IRMPD and DFT calculations that the structures most resembled an ion–dipole complex where the protonated amino acid interacts with the carbonyl end of the neutral amino acid, as was previously shown by a combination of thermochemical studies and DFT calculations.<sup>13</sup> Wu and McMahon<sup>30</sup> similarly demonstrated that the glycine molecules in the homogeneous proton-bound dimer were not zwitterionic, but they did provide results that presented the proline proton-bound dimer as being zwitterionic.

\* To whom all correspondence should be addressed at tfridgen@mun.ca.

The current study involves an investigation of the proton-bound glycine homodimer by IRMPD spectroscopy in the  $\sim 2400\text{--}3600\text{ cm}^{-1}$  spectral region, which is rich with N–H and O–H stretching modes. Complexes with the sodium ion and amino acids<sup>31–36</sup> are important in biological systems and have received much attention. A recent IRMPD study of oligoglycines and oligoalanines<sup>37</sup> bound to sodium ions showed that the presence of the sodium ion greatly affects the structure of the peptides and that sodium ion typically binds to three basic sites. Here, we also present the spectra of the sodium ion-bound dimer of glycine and thoroughly investigate possible structures for this ion with density functional calculations.

## 2. Methods

**2.1. Experimental Methods.** The details of the combination of the Bruker Apex Qe 7T Fourier transform ion cyclotron resonance mass spectrometer (FT-ICR-MS) with the Laser Vision infrared optical parametric oscillator/amplifier (OPO/OPA) has been described previously<sup>38</sup> and will not be repeated here. Proton-bound dimers of glycine were electrosprayed from a 0.1 mM solution of glycine in 18 M $\Omega$  (Millipore) water. The sodium ion-bound dimers were electrosprayed from the same solution to which a few drops of 1 mM NaCl were added. Following isolation in the ICR cell, ions were irradiated for 1–4 s with the OPO/OPA. If the wavelength of the IR laser radiation is in resonance with a vibrational mode, several photons are absorbed, leading to fragmentation of the proton- or sodium ion-bound dimer. The fragmentation pathways for both the proton- and sodium ion-bound dimers were solely loss of neutral glycine. After each irradiation event, a mass spectrum is recorded. The spectral width of the laser is estimated to be  $<5\text{ cm}^{-1}$ . The IRMPD efficiency is the negative logarithm of the fragment ion intensity divided by the sum of the fragment and precursor ion intensity.

**2.2. Computational Methods.** The Gaussian 03<sup>39</sup> program package was used. Structures were geometrically optimized using B3LYP hybrid density functional theory with a 6-31+G(d,p) basis set. Frequency calculations were also completed using this level of theory, which is notorious for providing excellent experimentally comparable infrared spectra combined with computational speed.<sup>40</sup> Because the raw harmonic vibrational frequencies produced at this level of theory are on average overestimated, various scaling factors have been proposed which are dependent upon the level of theory and the selected IR range.<sup>41</sup> The calculated frequencies used in this study were scaled by a factor of 0.955. They were furthermore convoluted with a Lorentzian profile having a  $5\text{ cm}^{-1}$  full width at half-maximum for presentation. A diverse selection of structures were evaluated and the lowest energy results, containing no imaginary vibrational frequencies, were considered. When attempting to match calculated one-photon spectra to experimental multiphoton spectra, minor deficiencies may arise which have been discussed elsewhere.<sup>42</sup>

Previous research has shown that for systems similar to those under study, there is a very minor effect on the relative energies when variations on the theoretical approaches are applied. In other words, relative B3LYP energies obtained from this calculation approach would be reasonably well converged with values from larger basis sets. The 298 K free energy differences are reported in comparison to the reported lowest-energy structure. Single point energy calculations were performed on each structure at the MP2(full)/6-311++G(2d,2p) level of theory. Thermochemical data and entropies were extracted from the initial DFT frequency calculation. This complete calculation

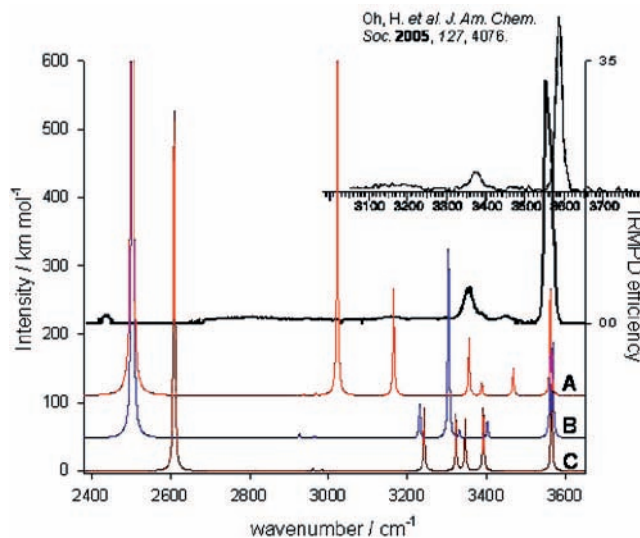


**Figure 1.** IRMPD spectrum of proton-bound glycine dimer in the  $2400\text{--}3600\text{ cm}^{-1}$  region. Also shown are the B3LYP/6-31+G(d,p) theoretical structures and corresponding infrared spectra for the three lowest energy structures. Labels A, B and C correspond to those in Figure 2.

approach was performed on all structures for both the proton- and sodium-bound glycine homodimers to determine the relative enthalpies and free energies. These energies are hence denoted as MP2(full)/6-311++G(2d,2p)//B3LYP/6-31+G(d,p).

## 3. Results and Discussion

**3.1. Glycine Proton-Bound Dimer.** The IRMPD spectrum of the proton-bound glycine dimer in the  $\sim 2400\text{--}3650\text{ cm}^{-1}$  region is shown in Figure 1. The B3LYP/6-31+G(d,p) predicted spectra for the three lowest-energy structures as determined by the optimizations are shown as well. Also in Figure 1 is the experimental spectrum determined by Oh et al.<sup>43</sup> over the  $3100\text{--}3700\text{ cm}^{-1}$  range. The spectra agree well, but the free O–H stretch is observed at  $\sim 3555\text{ cm}^{-1}$ , whereas in the Oh et al.<sup>43</sup> spectrum it is observed to be at about  $3590\text{ cm}^{-1}$ . Although we have no explanation for the discrepancy, we note that the free O–H stretch for neutral glycine is observed at  $3564\text{ cm}^{-1}$  in an argon matrix.<sup>2c,d</sup> Via a long-range through bond induction effect, the positive charge within the dimer would be expected to deplete electron density from the free O–H bond and red shift the position of the stretching vibration compared to the neutral and this shift is also predicted by the electronic calculations.

Before comparing the experimental and predicted spectra, it is interesting to compare the three lowest energy structures to which these spectra belong. Depicted in Figure 2 are the corresponding three lowest energy structures. The present energetic ordering agrees with that of previous studies.<sup>13,29</sup> The MP2/6-311++G(2d,2p)//B3LYP/6-31+G(d,p) enthalpies and free energies provided in Figure 2 are at 298 K and relative to structure A, which is found to be the most thermodynamically stable conformer. As determined previously,<sup>13,29</sup> the structure of the lowest energy conformer resembles an ion–dipole complex<sup>29</sup> involving N-protonated glycine bound to the carbonyl oxygen of the neutral amino acid. The binding proton resides closer to the amine N, a feature consistent with the most probable structure for protonated glycine.<sup>44</sup> There are also stabilizing intramolecular N–H $\cdots$ O and O–H $\cdots$ N hydrogen bonds within each amino acid moiety that are important aspects of the structure and show up in the infrared spectrum discussed below. Structure B was previously determined to be the lowest

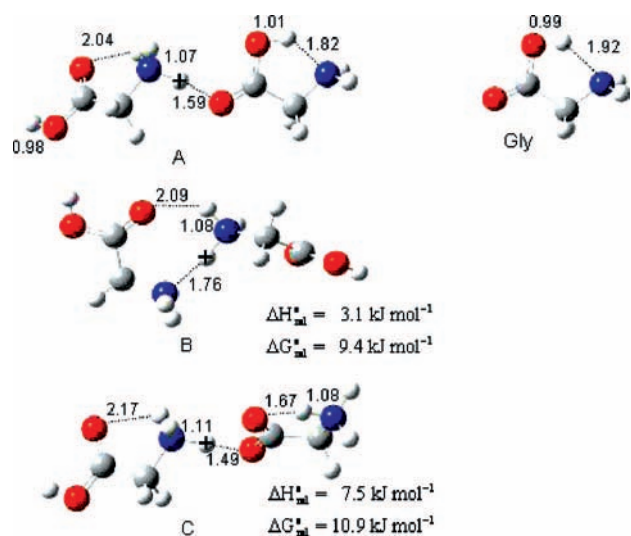


**Figure 2.** B3LYP/6-31+G(d,p) structures for the three lowest energy isomers of the glycine proton-bound dimer. Structure labels A, B, and C correspond to the predicted spectra in Figure 1. Bond lengths are in angstroms and the relative thermochemistries were calculated using MP2(full)/6-311++G(2d,2p)//B3LYP/6-31+G(d,p).

**TABLE 1: Table of Observed and Predicted Wavenumber Positions (Structure A) for the Glycine Proton-Bound Dimer**

observed position/cm <sup>-1</sup>	assignment	predicted <sup>a</sup> position (A)/cm <sup>-1</sup>
3555	free OH str	3562
3450	free NH <sub>2</sub> asym str	3438
3390 shoulder	free NH <sub>2</sub> sym str	3387
3360	non H-bonded N–H str	3355
2650–3300 very broad	H-bonded NH str/ H-bonded OH str	3165/ 3022
2440	shared proton str	2503

<sup>a</sup> B3LYP/6-31+G(d,p) scaled by 0.955.

energy conformer<sup>43,45</sup> where the proton binds the amino acids via the amino groups. This binding proton is significantly closer to one of the amino groups. There is also a N–H···O hydrogen bond between a carbonyl oxygen of one amino acid and the amino group of the other amino acid. This structure is higher in free energy by 9.4 kJ mol<sup>-1</sup>. Structure C, which is higher in free energy by 10.9 kJ mol<sup>-1</sup>, is similar to structure A; however, the hydroxyl hydrogen has been transferred to the amino group, resulting in a zwitterionic structure. In this case the binding proton shifts closer to the carboxyl oxygen than what is seen for structure A.

The experimental spectra are compared to the predicted spectra for structures A, B and C in Figure 1 and Table 1. Within the 3300–3650 cm<sup>-1</sup> region, the predicted spectrum for structure A clearly agrees best with the experimental spectrum. The free OH stretch observed at 3555 cm<sup>-1</sup> is fairly sharp and intense. The NH<sub>2</sub> asymmetric stretch for the free NH<sub>2</sub> group is observed at 3450 cm<sup>-1</sup>. The other fully resolved feature in this region is the non-hydrogen bonded N–H stretch (the left glycine) at 3360 cm<sup>-1</sup>. The shoulder on the high frequency side of this feature, at 3390 cm<sup>-1</sup>, is the free NH<sub>2</sub> symmetric stretch.

The band at 2440 cm<sup>-1</sup> is assigned to the shared proton asymmetric stretch. The predicted absorption is significantly to the blue of the observed feature. Harmonic calculations are not expected to adequately predict strongly anharmonic vibrations such as the shared proton asymmetric stretch. It has been seen in the past that shared proton stretches for heterogeneous proton bound dimers are observed at significantly lower frequency than

in the predicted spectra.<sup>46–48</sup> The glycine proton-bound dimer is expected to be transparent in this region of the infrared except for the shared-proton stretch, and this assignment is made with confidence. It would still be beneficial to observe the spectrum of the deuterium-labeled ion for confirmation of this assignment.

There are two bands predicted to occur at 3165 and 3022 cm<sup>-1</sup> corresponding to the hydrogen bonded N–H and O–H stretches, respectively. Although the experimental spectrum in this region may resemble noise, there is in fact an authentic broad absorption observed between ~2650 and 3300 cm<sup>-1</sup>. This is confirmed by blocking the laser radiation from the ICR cell, resulting in dissociation ceasing to occur. For neutral species which have strong intramolecular hydrogen bonds such as acetylacetone and malonaldehyde, for which the enol isomer is dominant, the strongly hydrogen bonded OH stretch is also observed to be very broad, occurring between 1800 and 3400 cm<sup>-1</sup> and lacking the intensity that harmonic calculations predict.<sup>49,50</sup> The broadness of this feature has been associated with the double-minimum type potential energy surface along the O–H–O stretching coordinate, strong anharmonicity, and strong coupling to low-frequency modes.<sup>50,51</sup> Progress has been made in attempts to model this anharmonic vibration by means of molecular dynamics calculations.<sup>52</sup> The broad bands in the present experimental spectrum between 2650 and 3300 cm<sup>-1</sup> are assigned to the hydrogen bonded N–H and O–H stretching modes.

It is worthwhile to compare the hydrogen bonded O–H stretch to that observed for the neutral in the similar conformation (see Figure 2), which has been observed to occur at 3200 cm<sup>-1</sup> in an argon matrix.<sup>2d</sup> Unscaled harmonic calculations place this vibrations at 3462 cm<sup>-1</sup> using MP2/aug-cc-pVDZ,<sup>53</sup> 3451 cm<sup>-1</sup> using B3LYP/aug-cc-pVDZ,<sup>2d</sup> and 3466 cm<sup>-1</sup> using B3LYP/6-31+G(d,p) for neutral glycine, as shown in Figure 2. Therefore, these calculations are all in agreement and would require a more extreme scaling factor (about 0.92) compared to the typical 0.96 for the “less anharmonic” vibrations. The B3LYP/6-31+G(d,p) structures of the proton-bound dimer and for neutral glycine, in Figure 2, reveal that the O–H–N hydrogen bond in the proton-bound dimer is significantly stronger, resulting in a longer O–H bond and would be expected to have an absorption that is red-shifted with respect to the neutral. In fact, the anharmonic vibration (B3LYP/6-31+G(d,p)) is predicted to occur at 3164 cm<sup>-1</sup> and, when scaled by a similarly extreme scaling factor would be 2910 cm<sup>-1</sup>, in reasonable agreement with the broad band observed in Figure 1.

The spectrum in Figure 1, along with the spectra in the 700–2000 cm<sup>-1</sup> region<sup>29,30</sup> represent a complete and assigned IR spectrum for the glycine proton-bound homodimer. These experiments, along with the thermochemical experiments<sup>13</sup> and the calculated thermochemistries, support the exclusive existence of structure A in the gas phase at 298 K. As mentioned previously, deuterium substitution experiments would be beneficial for this system.

**3.2. Sodium Ion-Bound Glycine Dimer.** The experimental IRMPD spectrum for the sodium ion-bound dimer of glycine from 3000 to 3700 cm<sup>-1</sup> is shown in Figure 3 along with the B3LYP/6-31+G(d,p) predicted spectra for the five lowest-energy structures as determined by the MP2/6-311++G(2d,2p)//B3LYP/6-31+G(d,p) energy calculations. The inset in Figure 3 is simply a repeat of the experiment in the NH<sub>2</sub> region with a slower scanning rate of the infrared laser. The predicted spectra for five isomers are also shown in Figure 3. The corresponding structures are depicted in Figure 4, along with the rest of the structures that have been deter-



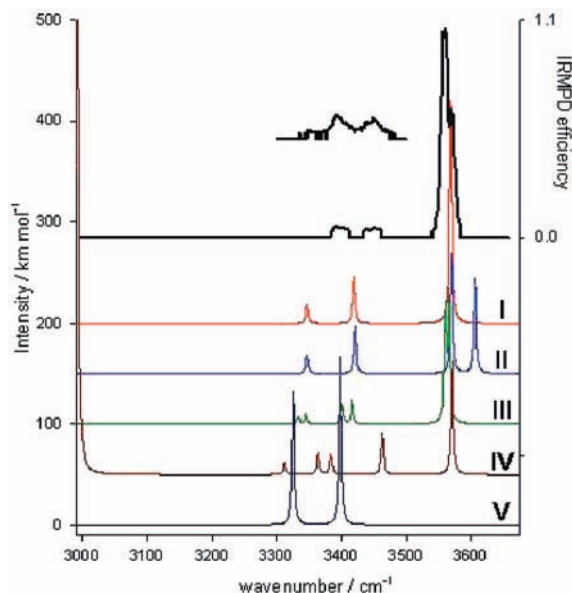


**Figure 3.** IRMPD spectrum of sodium ion-bound glycine dimer in the 3000–3700  $\text{cm}^{-1}$  region. Also shown are the B3LYP/6-31+G(d,p) theoretical structures and corresponding infrared spectra for the five lowest energy structures. Labels I–V correspond to those in Figure 4 and Table 3.

mined. The predicted thermochemistries associated with these structures are provided in Table 3.

Structure I is predicted to be the lowest in enthalpy and free energy by 20.8 and 20.0  $\text{kJ mol}^{-1}$ , respectively, over structure II. Structure I is symmetric and composed of two bidentate glycine ligands. This is consistent with the lowest energy glycine– $\text{Na}^+$  monomeric complex determined in previous studies.<sup>16,32,44,54</sup> Structure II is similar to structure I in that each amino acid is bidentate, bound to  $\text{Na}^+$  through the amine and carbonyl group. However, one of the OCOH dihedrals is rotated from  $0^\circ$  to about  $180^\circ$  such that the hydroxy hydrogen is sterically congesting a hydrogen on the  $\text{CH}_2$  group, probably accounting for most of the 20  $\text{kJ mol}^{-1}$  thermodynamic instability compared with structure I. Structure III differs from structure I in that there is a  $180^\circ$  rotation about the C–C bond so that the hydroxy oxygen on one amino acid is interacting with  $\text{Na}^+$  rather than the carbonyl oxygen. There also exist two structures related to II and III (IIa and IIIa, also shown in Figure 4) that are the symmetric versions and are significantly higher in energy than II and III. Structure IV is similar to the lowest energy glycine proton-bound dimer that was discussed above. The zwitterionic structure, V, is the next highest in energy, nearly 40  $\text{kJ mol}^{-1}$  higher than I. The rest of the structures are presented (as well as I–V) in Figure 4 and their relative enthalpies and free energies in Table 3.

The IRMPD spectrum for the sodium ion-bound dimer of glycine (Figure 3) is not as rich as that for the proton-bound dimer, consisting of three main features. The O–H stretch is observed at 3560  $\text{cm}^{-1}$  and the asymmetric and symmetric  $\text{NH}_2$  stretching absorptions are observed at 3450 and 3390  $\text{cm}^{-1}$ , respectively (see also Table 2). These bands are, of course, doubly degenerate, and the band positions are virtually identical to those observed for the proton-bound glycine dimer.

The predicted spectrum for structure I compares more favorably with the experimental IRMPD spectrum than any of the higher energy isomers. It should be noted, however, that we cannot rule out the other structures solely on the basis of the IRMPD spectrum. For example, structure III (or even IIIa)

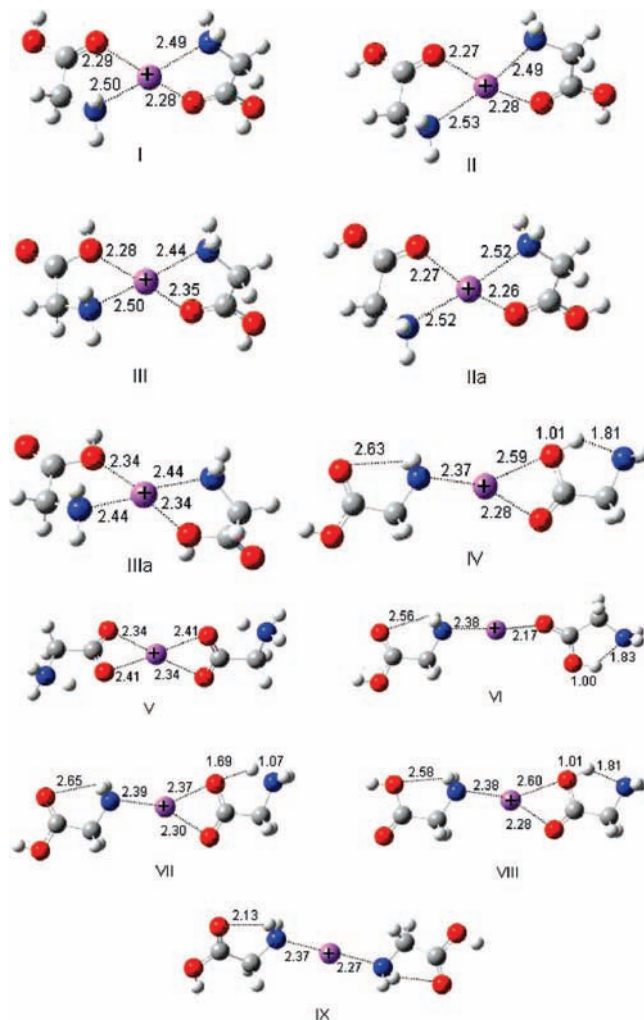


**Figure 4.** B3LYP/6-31+G(d,p) structures for isomers of the glycine sodium ion-bound dimer. Structure labels I–V correspond to the predicted spectra in Figure 3. The relative thermochemistries of all structures, calculated using MP2(full)/6-311++G(2d,2p)//B3LYP/6-31+G(d,p), are provided in Table 3.

**TABLE 2: Table of Observed and Predicted Wavenumber Positions (Structure I) for the Glycine Sodium Ion-Bound Dimer**

observed position/ $\text{cm}^{-1}$	assignment	predicted <sup>a</sup> position (I) <sup>b</sup> / $\text{cm}^{-1}$
3560	OH str	3569
3450	$\text{NH}_2$ asym str	3419
3390	$\text{NH}_2$ sym str	3347

<sup>a</sup> B3LYP/6-31+G(d,p) scaled by 0.955. <sup>b</sup> Note that these predicted bands are doubly degenerate due to the symmetry of the sodium ion-bound dimer.

cannot be completely ruled out by comparison of its predicted infrared spectrum with the experimental work; however, it is predicted to be higher in energy by 30.1  $\text{kJ mol}^{-1}$ , which would mean that its contribution to a mixture would be minimal. Structures II and IIa can be ruled out on the basis of the predicted position of the free OH stretching vibration(s) that would occur at significantly higher energy than that observed. Structure IV can probably be ruled out on the basis of the number of bands observed because the predicted spectrum is significantly more complicated in this region. Although the predicted spectrum for the zwitterionic structure V does not agree with the experimental spectrum because an O–H stretch

**TABLE 3: 298 K Thermochemistries<sup>b</sup> of Sodium Ion-Bound Dimers of Glycine<sup>a</sup>**

structure	relative enthalpy <sup>b</sup> /kJ mol <sup>-1</sup>	relative free energy <sup>b</sup> /kJ mol <sup>-1</sup>
I	0	0
II	20.8	20.0
IIa	41.4	39.8
III	30.0	30.1
IIIa	60.6	60.6
IV	49.5	38.1
V	37.0	38.4
VI	51.5	38.6
VII	55.1	47.3
VIII	61.6	51.1
IX	122.8	104.7

<sup>a</sup> Labels I–IX correspond to those in Figures 3 and 4. <sup>b</sup> MP2-(full)/6-311++G(2d,2p)//B3LYP/6-31+G(d,p).

is observed, the observation of the O–H stretch in the experimental spectrum does not preclude V from existing in the mixture because the NH<sub>2</sub> stretching vibrations still occur at roughly the same position as in the lowest energy isomer. However, all the higher energy structures we have reported are significantly higher in enthalpy and free energy by between 20 and 105 kJ mol<sup>-1</sup> than the lowest energy structure and are not likely important. Thermochemical studies would be beneficial and might provided further evidence for one or a mixture of structures. The IRMPD spectrum presented agrees with that predicted for the lowest energy structure, which is consistent with and confirms the results of the thermochemical calculations.

#### 4. Conclusions

The IRMPD spectrum of the proton bound dimer of glycine was extended to 2400 cm<sup>-1</sup> from a previously published spectrum<sup>43</sup> whose low energy limit was ~3100 cm<sup>-1</sup>. This extension allowed for the observation and assignment of the shared proton stretch at 2440 cm<sup>-1</sup> and the hydrogen bonded O–H and N–H stretching vibrations, which is a weak and very broad feature spanning ~2650–3300 cm<sup>-1</sup>. The fragmentation was confirmed to as being dissociation induced by the OPO laser because it ceased to occur when the laser radiation was blocked. The present spectrum also allowed the assignment of the free O–H stretch, the NH<sub>2</sub> symmetric and asymmetric stretching vibrations, and the N–H stretch corresponding to non-hydrogen bonded NH. The experimental IRMPD spectrum clearly allows the assignment of the structure of the glycine proton-bound dimer to the ion–dipole complex and rules out any of the higher energy structures. The calculated region below 3300 cm<sup>-1</sup> cannot easily be accurately modeled due to the anharmonic nature of these hydrogen bonded modes.

The IRMPD spectrum for the sodium ion-bound dimer of glycine is a much simpler spectrum, consisting of three bands that coincide very well with the positions of the same modes for the proton-bound dimer. Unlike the glycine proton-bound dimer, where agreement between the experimental and theoretical spectra provided a more definite assignment of structure, the IRMPD spectrum alone cannot be used to rule out all structures. However, the electronic structure calculations show that the lowest energy structure is such by some 20 kJ mol<sup>-1</sup>. The experimental spectrum is consistent with the predicted spectrum for the lowest energy structure. This leads to the conclusion that the sodium ion-bound dimer is composed of two glycine molecules bound in a bidentate fashion through the carbonyl oxygen and the amino nitrogen and that glycine monomers are non-zwitterionic.

**Acknowledgment.** We are grateful for the generous financial support of our work by the Natural Sciences and Engineering Research Council of Canada (NSERC). E.A.L.G. acknowledges the CGS-M granted by NSERC. The financial support of the European Commission through EPITOPES is also gratefully acknowledged as is the technical assistance of T. Besson and P. Maitre. MBB and JLC and the referees are thanked for their help in editing the manuscript.

#### References and Notes

- (1) Levy, H. A.; Corey, R. B. *J. Am. Chem. Soc.* **1941**, *63*, 2095.
- (2) (a) Stepanian, S. G.; Reva, I. D.; Radchenko, E. D.; Rosado, M. T. S.; Duarte, M. L. T. S.; Fausto, R.; Adamowicz, L. *J. Phys. Chem. A* **1998**, *102*, 1041. (b) Stepanian, S. G.; Reva, I. D.; Radchenko, E. D.; Adamowicz, L. *J. Phys. Chem. A* **1998**, *102*, 4623. (c) Stepanian, S. G.; Reva, I. D.; Radchenko, E. D.; Rosado, M. T. S.; Duarte, M. L. T. S.; Fausto, R.; Adamowicz, L. *J. Phys. Chem. A* **1998**, *102*, 1041. (d) Stepanian, S. G.; Reva, I. D.; Radchenko, E. D.; Adamowicz, L. *J. Phys. Chem. A* **1999**, *103*, 4404.
- (3) (a) Blanco, S.; Lesarri, A.; Lopez, J. C.; Alonso, J. L. *J. Am. Chem. Soc.* **2004**, *126*, 11675. (b) Lesarri, A.; Cocinero, E. J.; Lopez, J. C.; Alonso, J. L. *Angew. Chem., Int. Ed.* **2004**, *120*, 6191.
- (4) (a) Godfrey, P. D.; Brown, R. D. *J. Am. Chem. Soc.* **1995**, *117*, 2019. (b) Godfrey, P. D.; Firth, S.; Hatherley, L. D.; Brown, R. D.; Pierlot, A. P. *J. Am. Chem. Soc.* **1993**, *115*, 9687.
- (5) Csaszar, A. G.; Perczel, A. *Prog. Biophys. Mol. Biol.* **1999**, *71*, 243.
- (6) Ding, Y.; Krogh-Jespersen, K. *Chem. Phys. Lett.* **1992**, *199*, 261.
- (7) Jensen, J. H.; Gordon, M. S. *J. Am. Chem. Soc.* **1995**, *117*, 8159.
- (8) Ahn, D.; Park, S.; Jeon, I.; Lee, M.; Kim, N.; Han, Y.; Lee, S. *J. Phys. Chem. B* **2003**, *107*, 14109.
- (9) Bachrach, S. M. *J. Phys. Chem. A* **2008**, *112*, 3722.
- (10) Xu, S.; Nilles, J. M.; Bowen, K. H. *J. Chem. Phys.* **2003**, *119*, 10696.
- (11) Alberty, R. A. *Biophys. Chem.* **2007**, *125*, 328.
- (12) Wu, R.; McMahon, T. B. *J. Am. Chem. Soc.* **2008**, *130*, 3722.
- (13) Raspopov, S. A.; McMahon, T. B. *J. Mass Spectrom.* **2005**, *40*, 1536.
- (14) Lioe, H.; O'Hair, R. A. J.; Gronert, S.; Austin, A.; Reid, G. E. *Int. J. Mass Spectrom.* **2007**, *267*, 220.
- (15) Jones, C. M.; Bernier, M.; Carson, E.; Colyer, K. E.; Metz, R.; Pawlow, A.; Wischow, E. D.; Webb, I.; Andriole, E. J.; Poustma, J. C. *Int. J. Mass Spectrom.* **2007**, *267*, 54.
- (16) Wyttenbach, T.; Witt, M.; Bowers, M. T. *J. Am. Chem. Soc.* **2000**, *122*, 3548.
- (17) Shoeib, T.; Siu, K. W. M.; Hopkinson, A. C. *J. Phys. Chem. A* **2002**, *106*, 6121.
- (18) Wang, P.; Ohanessian, G.; Wesdemiotis, C. *Int. J. Mass Spectrom.* **2008**, *269*, 34.
- (19) Marino, T.; Russo, N.; Toscano, M. *J. Phys. Chem. B* **2003**, *107*, 2588.
- (20) Zhao, J.; Siu, K. W. M.; Hopkinson, A. C. *Phys. Chem. Chem. Phys.* **2008**, *10*, 281.
- (21) Armentrout, P. B.; Rodgers, M. T.; Oomens, J.; Steill, J. D. *J. Phys. Chem. A* **2008**, *112*, 2248.
- (22) Bush, M. F.; O'Brien, J. T.; Prell, J. S.; Saykally, R. J.; Williams, E. R. *J. Am. Chem. Soc.* **2007**, *129*, 1612.
- (23) Dunbar, R. C.; Polfer, N. C.; Oomens, J. *J. Am. Chem. Soc.* **2007**, *129*, 14562.
- (24) Forbes, M. W.; Bush, M. F.; Polfer, N. C.; Oomens, J.; Dunbar, R. C.; Williams, E. R.; Jockusch, R. A. *J. Phys. Chem. A* **2007**, *111*, 11759.
- (25) Jockusch, R. A.; Price, W. D.; Williams, E. R. *J. Phys. Chem. A* **1999**, *103*, 9266.
- (26) Jockusch, R. A.; Lemoff, A. S.; Williams, E. R. *J. Phys. Chem. A* **2001**, *105*, 10929.
- (27) Lemoff, A. S.; Williams, E. R. *J. Am. Soc. Mass Spectrom.* **2004**, *15*, 1014.
- (28) Bush, M. F.; Prell, J. S.; Saykally, R. J.; Williams, E. R. *J. Am. Chem. Soc.* **2007**, *129*, 13544.
- (29) Rajabi, K.; Fridgen, T. D. *J. Phys. Chem. A* **2008**, *112*, 23.
- (30) Wu, R.; McMahon, T. B. *J. Am. Chem. Soc.* **2007**, *129*, 4864.
- (31) Wang, P.; Wesdemiotis, C.; Kapota, C.; Ohanessian, G. *J. Am. Soc. Mass Spectrom.* **2007**, *18*, 541.
- (32) Moision, R. M.; Armentrout, P. B. *J. Phys. Chem. A* **2002**, *106*, 10350.
- (33) Kish, M. M.; Wesdemiotis, C.; Ohanessian, G. *J. Phys. Chem. B* **2004**, *108*, 3086.
- (34) Cerda, B. A.; Hoyau, S.; Ohanessian, G.; Wesdemiotis, C. *J. Am. Chem. Soc.* **1998**, *120*, 2437.
- (35) Dunbar, R. C. *J. Phys. Chem. A* **2000**, *104*, 8067.

- (36) Kapota, C.; Lemaire, J.; Maitre, P.; Ohanessian, G. *J. Am. Chem. Soc.* **2004**, *126*, 1836.
- (37) Balaj, O.-P.; Kapota, C.; Lemaire, J.; Ohanessian, G. *Int. J. Mass Spectrom.* **2008**, *269*, 196.
- (38) Bakker, J. M.; Besson, T.; Lemaire, J.; Scuderi, D.; Maitre, P. *J. Phys. Chem. A* **2007**, *111*, 13415.
- (39) Frisch, M. J.; Trucks, G. W.; Schlegel, H. B.; Scuseria, G. E.; Robb, M. A.; Cheeseman, J. R.; Montgomery, J. A., Jr.; Vreven, T.; Kudin, K. N.; Burant, J. C.; Millam, J. M.; Iyengar, S. S.; Tomasi, J.; Barone, V.; Mennucci, B.; Cossi, M.; Scalmani, G.; Rega, N.; Petersson, G. A.; Nakatsuji, H.; Hada, M.; Ehara, M.; Toyota, K.; Fukuda, R.; Hasegawa, J.; Ishida, M.; Nakajima, T.; Honda, Y.; Kitao, O.; Nakai, H.; Klene, M.; Li, X.; Knox, J. E.; Hratchian, H. P.; Cross, J. B.; Adamo, C.; Jaramillo, J.; Gomperts, R.; Stratmann, R. E.; Yazyev, O.; Austin, A. J.; Cammi, R.; Pomelli, C.; Ochterski, J. W.; Ayala, P. Y.; Morokuma, K.; Voth, G. A.; Salvador, P.; Dannenberg, J. J.; Zakrzewski, V. G.; Dapprich, S.; Daniels, A. D.; Strain, M. C.; Farkas, O.; Malick, D. K.; Rabuck, A. D.; Raghavachari, K.; Foresman, J. B.; Ortiz, J. V.; Cui, Q.; Baboul, A. G.; Clifford, S.; Cioslowski, J.; Stefanov, B. B.; Liu, G.; Liashenko, A.; Piskorz, P.; Komaromi, I.; Martin, R. L.; Fox, D. J.; Keith, T.; Al-Laham, M. A.; Peng, C. Y.; Nanayakkara, A.; Challacombe, M.; Gill, P. M. W.; Johnson, B.; Chen, W.; Wong, M. W.; Gonzalez, C.; Pople, J. A. *Gaussian 03*, Revision C.02; Gaussian, Inc.: Wallingford, CT, 2004.
- (40) Andersson, M. P.; Uvdal, P. *J. Phys. Chem. A* **2005**, *109*, 2937.
- (41) Scott, A. P.; Radom, L. *J. Phys. Chem.* **1996**, *100*, 16502.
- (42) Oomens, J.; Sartakov, B. G.; Meijer, G.; von Helden, G. *Int. J. Mass Spectrom.* **2006**, *254*, 1.
- (43) Oh, H.; Lin, C.; Hwang, H. Y.; Zhai, H.; Breuker, K.; Zabrouskov, V.; Carpenter, B. K.; McLafferty, F. W. *J. Am. Chem. Soc.* **2005**, *127*, 4076.
- (44) Jensen, F. *J. Am. Chem. Soc.* **1992**, *114*, 9533.
- (45) Price, W. D.; Schnier, P. D.; Williams, E. R. *J. Phys. Chem. B* **1997**, *101*, 664.
- (46) Burt, M. B.; Fridgen, T. D. *J. Phys. Chem. A* **2007**, *111*, 10738.
- (47) Fridgen, T. D.; MacAleese, L.; Maitre, P.; McMahon, T. B.; Boissel, P.; Lemaire, J. *Phys. Chem. Chem. Phys.* **2005**, *7*, 2747.
- (48) Fridgen, T. D.; MacAleese, L.; McMahon, T. B.; Lemaire, J.; Maitre, P. *Phys. Chem. Chem. Phys.* **2006**, *8*, 955.
- (49) (a) Chiavassa, T.; Roubin, P.; Pizzala, L.; Verlaque, P.; Allouche, A.; Marinelli, F. *J. Phys. Chem.* **1992**, *96*, 10659. (b) Chiavassa, T.; Verlaque, P.; Pizzala, L.; Roubin, P. *Spectrochim. Acta* **1994**, *50A*, 343.
- (50) Matanovic, I.; Doslic, N. *J. Phys. Chem. A* **2005**, *109*, 4185.
- (51) Tayyari, S. F.; Zeegers-Huyskens, Th.; Wood, J. L. *Spectrochim. Acta* **1979**, *35A*, 1289.
- (52) Jezierska, A.; Panek, J. *J. Chem. Theory Comput.* **2008**, *4*, 375.
- (53) Bludsky, O.; Chocholousova, J.; Vacek, J.; Huisken, F.; Hobza, P. *J. Chem. Phys.* **2000**, *113*, 4629.
- (54) Hoyau, S.; Ohanessian, G. *Chem. Eur. J.* **1998**, *4*, 1561.

JP805514B